Indian Geotechnical Journal, 39(4), October 2009, 341-359

Bearing Capacity of Strip Footing on Two Layered Clays under Combined Loading

Tsuyoshi Takayanagi*, Jun Izawa and Osamu Kusakabe*****

Introduction

The problem of bearing capacity of footing on two clay layered ground has a long history of research, starting from a classical solution for vertical bearing capacity of strip footing by limit equilibrium analysis, using circular slip surface by Button (1953). He adopted two parameters to describe the problem; the ratio of undrained shear strength of the bottom clay layer (c_b) to that of the top layer (c_t), and the ratio of depth measured from the base of footing to the interface of the two layers (D) to half of footing width (B/2) and provided design charts in terms of bearing capacity factor, N_c, for two cases: (a) stiff clay overlying soft clay and (b) soft clay overlying stiff clay. Reddy and Srinivasan (1967) extended this analysis to anisotropic clays with a linear variation of shear strength with depth. Brown and Meyerhof (1969) criticized the use of circular slip surface based on a number of laboratory loading tests using strip and circular footings on various combinations of two layered clays, and provided charts for modified bearing capacity factors in terms of undrained shear strength ratio, c_b/c_t, and depth of top layer/footing width ratio, D/B. Purshothamaraj et al. (1974) analyzed the vertical bearing capacity problem on two layered ground with cohesive-frictional soils based on the upper bound theorem. Chen (1975) also analyzed the Button's problem from the context of limit analysis using a rotational mechanism. Nakase et al.(1987) conducted a series of centrifuge tests on normally consolidated clay layer with a surface crust layer with upper bound analyses. Florkiewicz (1989) proposed the kinematic approach of limit analysis for an inclined layered ground with Mohr-Coulomb materials, using rigid block collapse mechanism of two-layer soil. He then compared his analytical results with experimental data by Meyerhof and Hanna (1978) and Hanna (1981) and also with upper bound solutions by Chen (1975). Michalowski and Shi (1995) adopted the similar kinematic approach to calculate the average limit pressure under strip footing. The method is applicable to any combination of parameters of the two layers, but the results are presented only for

* Researcher, Geotechnical Hazard and Risk Mitigation, Japan Railway Technical Research Institute 2-3-38 Hikari-cho, Kokubunji-shi, Tokyo 185-8540, Japan, Tel: +81-42-573-7263, Fax: +81-42-573-7398, e-mail: yanagi@rtri.or.jp

** Assistant Professor, Department of Civil Engineering, Tokyo Institute of Technology, 2-12-1 Oh-okayama, Meguro-ku, Tokyo 152-8552, Japan, Tel: +81-3-5734-2798, Fax: +81-3-5734-3577, e-mail:jizawa@cv.titech.ac.jp

*** Professor, Department of Civil Engineering, Tokyo Institute of Technology, 2-12-1 Oh-okayama, Meguro-ku, Tokyo 152-8552, Japan, Tel: +81-3-5734-2798, Fax: +81-3-5734-3577, e-mail:kusakabe@cv.titech.ac.jp

a specific case when a footing is placed on a layer of granular soil resting on clay. Merifield et al.(1999) applied numerical limit analysis to evaluate the undrained bearing capacity of a rigid surface strip footing resting on a two-layer clay deposit. Rigorous bounds on the ultimate bearing capacity are obtained by employing finite elements in conjunction with the upper and lower bound limit theorems of classical plasticity. Michalowski (2002) presented upper bound solutions to limit loads on strip footing over two-layer clay foundation soil, considering two failure mechanisms: one with a continually deforming field and the other with a multi-block mechanism. He then found that the multi-block mechanism yields the least upper bound. The method was also used for calculations of bearing capacity of strip footings subjected to loads with horizontal components. Wang and Carter (2002) conducted large deformation 2D FE analyses with the Arbitrary Lagrangian-Eulerain method on deep penetration behaviour of strip and circular footings overlying two different undrained clay layers, where the upper layer was always stronger than the lower layer. They reported that the movement of soil from beneath the footing significantly affects the bearing response. Zhu & Michalowski (2005) performed three dimensional finite element analyses for bearing capacity of rectangular footings on two-layer clay. More recently Kim et al. (2008) reported 1 g model test, looking into the problem of bearing capacity evaluation in the early stage of ground improvement in marine clay dredged deposits. They concluded that Brown & Meyerhof equation underestimated and Button equation overestimated the experimental results. From the literature survey, it has been understood that all the previous studies on two layered cohesive layer except Michalowski (2002), are related to vertical bearing capacity.

Over a few decades it has been known that there is a surface in load space that defines a failure envelop for the footing, which can be written in the form of $f(V/s_uA, H/s_uA, M/s_uAB)=0$, where V, H and M are vertical load, horizontal load and moment, respectively, and A is the plan area of the footing, B is the width of the footing and s_u is the undrained shear strength of the soil beneath the base of the footing. The common sign conventions for loads and moments used are based on the right-handed axes and clockwise positive conventions, as is shown in Figure 1.

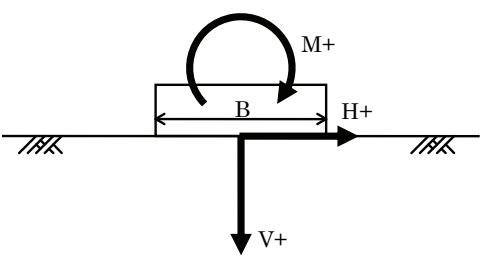

Fig. 1 The Common Sign Conventions for Loads and Moments

The effective width concept proposed by Meyerhof (1953) gives a failure envelop of footing under vertical and moment loading. Bolton (1979) presented a theoretical expression for vertical bearing capacity of a strip footing subjected to an inclined load. Recently finite element studies have been conducted for a footing on clay subjected to combined vertical, moment and horizontal loading. Bransby and Randolph (1998) conducted two dimensional finite element analyses, assuming that the clay obeys an elastic-plastic Tresca material with undrained shear strength

linearly increasing with depth. The footing was assumed to adhere fully to the soil, which enables to develop compressive, tensile and shear stresses at the interface between the footing and the soil. Based on soil displacement fields by FEM, they developed upper bound mechanisms; wedge, scoop and combinations of them, as are illustrated in Figure 2.

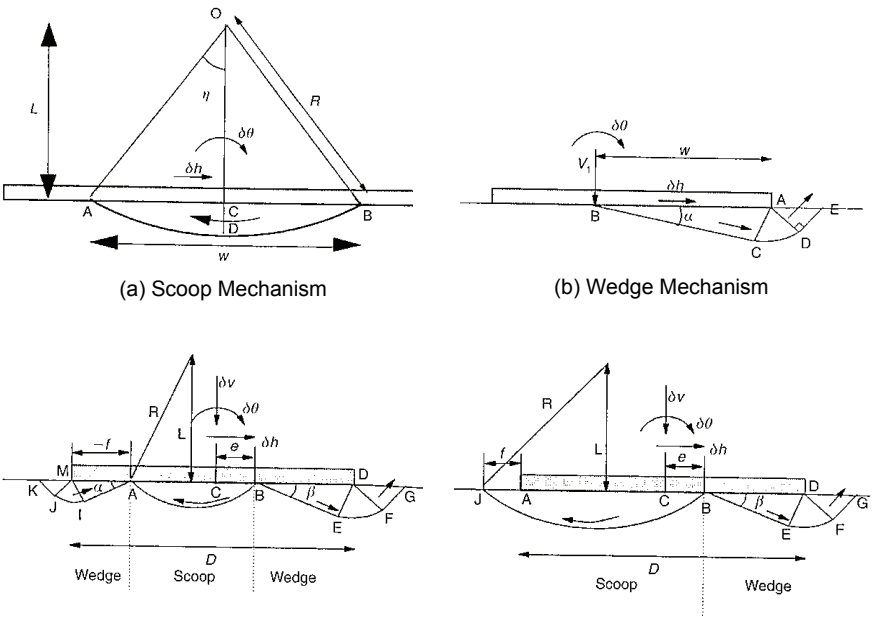

(a) Scoop Mechanism

(b) Wedge Mechanism

(c) Wedge-Scoop-Wedge Mechanism

(d) Scoop-Wedge Mechanism

Fig. 2 Component Upper Bound Plasticity Mechanisms (Bransby & Randolph, 1998)

They found that the shape of the failure envelop was found to be similar to that predicted by previous workers in V-M and V-H space but differed significantly in M-H space. That is, the failure envelop in M-H space is not symmetric, depending on the sign conventions of M and H. The combination of positive moment and negative horizontal load develops a simple scoop failure, whereas the combination of positive moment and positive horizontal load generates the wedge-scoop-wedge mechanism, resulting in the soil outside the footing base being pulled up sideways due to the adhesion between the footing base and the soil, associated with further mobilization of shear strength of the soil outside the footing base. Taiebat and Carter (2000) carried out three-dimensional finite-element analyses of circular footing on the surface of homogeneous, purely cohesive soil, under the similar assumption as those of Bransby and Randolph (1998). A three-dimensional failure locus was presented, and an equation that approximates the shape of the failure locus was also suggested as

$$F = \left(\frac{V}{V_u}\right) + \left[\frac{M}{M_u}\left(1 - \alpha\frac{HM}{H_u|M|}\right)\right]^2 + \left|\left(\frac{H}{H_u}\right)^3\right| - 1 = 0 \qquad (1)$$

where α is a factor that depends on the soil profile, and V_u, M_u and H_u represents the capacity of the footing under pure vertical load, pure moment and pure horizontal load, respectively. They concluded that overall the approximation is satisfactory, and the equation gives conservative and sufficient results for many practical applications. These studies are related to either a single clay layer of uniform strength or normally consolidated.

This paper is a finite element study of bearing capacity of strip footing on two cohesive layered deposits, subjected to a vertical, horizontal and moment combined loading.

Method of FEM Analysis

Figure 3 shows a typical finite-element mesh in the plane strain condition. The ground was assumed to be a level ground with two horizontally layered cohesive deposits. The footing width (B) was taken to be 160mm, referring to the experimental study conducted by Brown and Meyerhof (1969) and the area of analysis was about 9B in width and 2.5B in depth, to minimize possible boundary effects, although their experimental study used a box of 700mm in width and 320mm in depth. At the boundaries, the vertical and horizontal displacements at the bottom boundary were fixed, as were the horizontal displacements at the side boundaries. The footing base was assumed to be adhering fully to the soil.

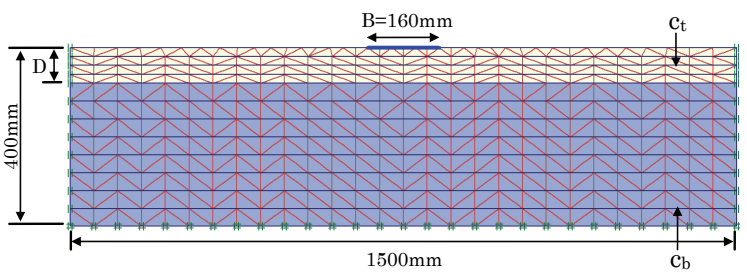

Fig. 3 Typical FE Mesh used

The element used was a 15-node triangle. The element stiffness matrix was evaluated by numerical integration using a total of 12 Gauss points. There were 684 elements, 5657 nodes and 8208 Gauss points in the mesh shown in Figure 3. The program used was a commercially available two-dimensional FEM program, Plaxis version 8 (Brinkgreve, R.B.J., 2002).

Since undrained bearing failure was considered in this study, the soil was assumed to be an elastic perfectly plastic material, obeying Tresca failure criterion. Two groups of layered ground were studied: (a) stiff clay overlying soft clay and (b) soft clay overlying stiff clay. The undrained shear strength of stiff clay was assumed to be a fixed value of 80 kN/m^2 and the undrained shear strength of soft clay varied from 20 to 60 kN/m^2, covering the values of c_b/c_t ratio from 0.25 to 0.75 for the cases of stiff clay overlying soft clay, and from 1.33 to 4.0 for the cases of soft clay overlying stiff clay.

The effect of two layered ground is expressed by the D/B ratio. The value of D/B varies from 0 to 2.0. In total, 51 cases were calculated. The values of other geotechnical parameters used for the FEM analysis are listed in Table 1.

Table 1 Input Parameters

Unit weight	Young's modulus	Undrained shear strength		Poisson's ratio
		for stiff clay	for soft clay	
γ(kN/m^3)	E(kN/m^2)	(kN/m^2)	(kN/m^2)	ν
16	50,000	80	20, 40, 60	0.495

Numerical procedures can be described as follows, taking an example for the case of H-V combined loading. A loading path was selected to maintain a constant value of H/V. The load increment was automatically decided with trial calculation in the program. The calculation was terminated when the load increment automatically specified by the program was negative twice in succession. About 10 loading paths were selected for each case to establish the shape of failure surface in H and V space. Identical procedures were carried out for M-V and H-M combined loadings.

Results and Discussion

Bearing Capacity of Footing on Stiff Clay Overlying Soft Clay: $C_b/C_t<1$

Failure Surface on V-H Plane

Figure 4 plots the value of H/s_uA against V/s_uA at failure for various values of D/B in the range from 0 to 2 for the case of $c_b/c_t=0.25$, where s_u is equal to the undrained shear strength of the top clay layer, c_t, and A is the bottom plan of the footing (A=B*1).

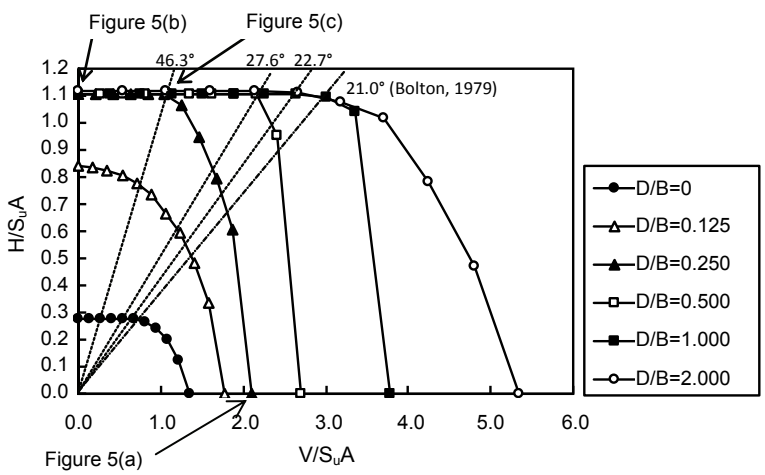

Fig. 4 Failure Envelopes in H-V Space ($C_b/C_t=0.25$)

The case of D/B=0 corresponds to the single clay layer with the undrained shear strength of the bottom layer, c_b. V/s_uA can be regarded as bearing capacity factor, N_c. The value of V/s_uA at the horizontal axis (under pure vertical loading) is 5.38 for D/B=2.0 and 1.34 for D/B=0, four times difference between the two, as was expected from the condition of c_b/c_t=0.25. The value of H/s_uA at the vertical axis (under pure horizontal loading) is 1.1 for D/B=2.0 and 0.3 for D/B=0, once again four times difference. Hereafter the value of V at the horizontal axis and the value of H at the vertical axis are denoted as V_u and H_u, respectively for a given D/B value.

Although the bearing capacity factor N_c obtained is about 5% larger than the plastic solution of $(2 + \pi)$, it is considered that the present study provides the consistent results and normalized values of V/V_u and H/H_u gives meaningful practical information.

Under the combined loading conditions, any horizontal load results in a drop of vertical resistance with an abrupt drop in vertical resistance, when the angle of loading inclination, defined by $\tan^{-1}(H/V)$ becomes around 20° for the case of D/B=0 and 2.0. This result is very much consistent with the value of 21° for a single clay layer theoretically derived by Bolton (1979). Vertical bearing capacity (V_u) is sensitively influenced by existence of the bottom soft clay layer, resulting in significant decrease when D/B decreases. In contrast, the horizontal bearing capacity (H_u) remains unaffected until D/B value becomes smaller than 0.25. It is seen that the values for D/B=1.0, 0.5 and 0.25 are identical to those of D/B=2.0 until the angle of loading inclination becomes around 22.7°, 27.6°, 46.3°, respectively.

The change of bearing capacity is always associated with the change in failure mode. Figures 5(a), 5(b) & 5 (c) show three displacement fields with different angles of loading inclination. As the angel of loading inclination increases, the failure mode changes from classical indentation mode to the wedge mode and finally to the slip mode where the slip surface is formed just beneath the footing.

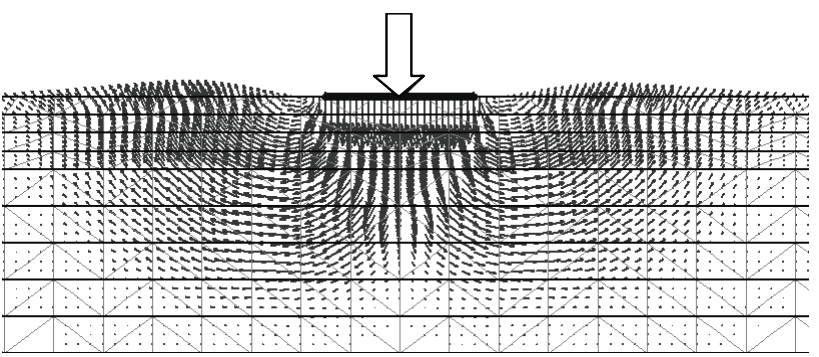

Fig. 5 (a) Failure Mode for Pure Vertical Loading (Scale Factor=2)
(D/B=0.25, c_b/c_t=0.25)

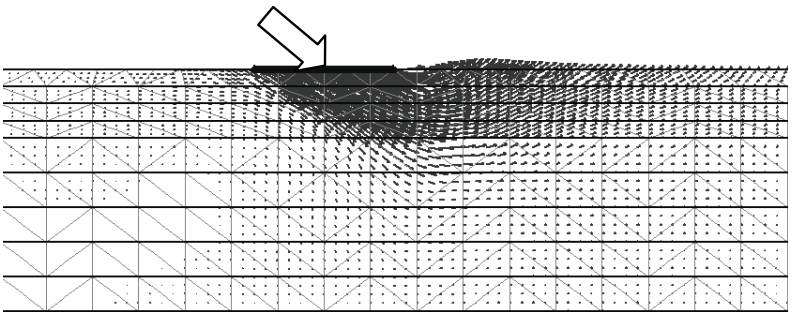

Fig. 5 (b) Failure Mode for Loading Inclination: $\tan^{-1}(V/H) = 46.3°$ (Scale Factor=20)
($D/B=0.25$, $c_b/c_t=0.25$)

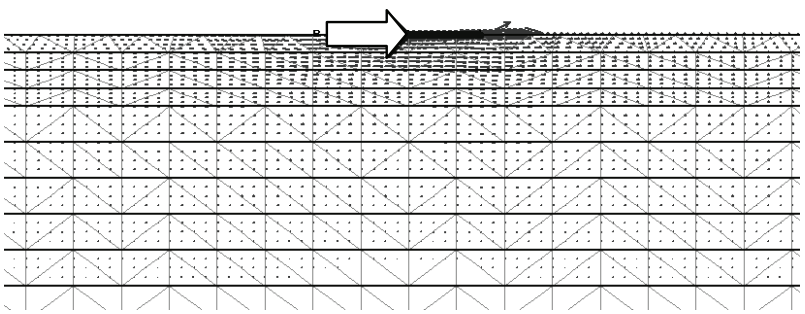

Fig. 5 (c) Failure Mode for Pure Horizontal Loading (Scale Factor=20)
($D/B=0.25$, $c_b/c_t=0.25$)

The normalized form of failure envelop, H/H_u-V/V_u space, is presented in Figure 6. The normalized failure envelops for D/B=2.0 and 0 are identical, both of which corresponds to the problems of the single clay layer. As D/B increases from D/B=0, the failure envelop first shrinks and then starts expanding until D/B becomes 1.0, and it shrinks again towards that of single clay layer.

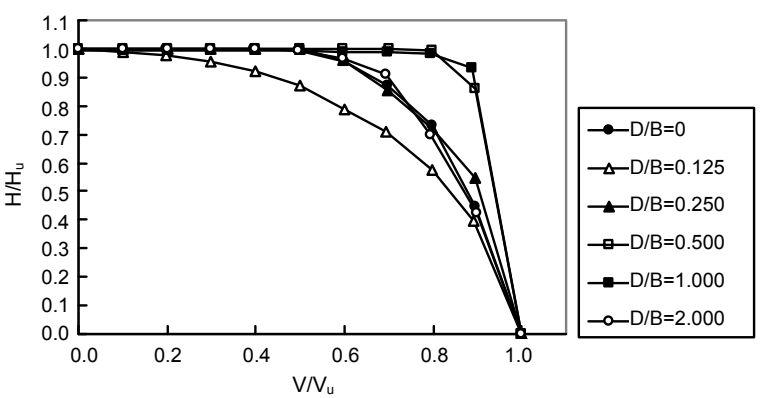

Fig. 6 Normalised Failure Envelopes in H–V Space ($c_b/c_t=0.25$)

Failure Surfaces on V-M Plane and H-M Plane

Figure 7 plots the value of M/s_uAB against V/s_uA at failure for various values of D/B in the range from 0 to 2.0 for the case of c_b/c_t=0.25. The value of M/s_uAB is 0.822 for D/B=2.0 and 0.205 for D/B=0, once again four times difference. Under the V-M combined loading conditions, any moment load results in a gradual drop of vertical resistance. It is noted that the values for D/B=1.0 are identical to those of D/B=2.0 until the angle defined by $\tan^{-1}(M/B/V)$ becomes around 16.6°.

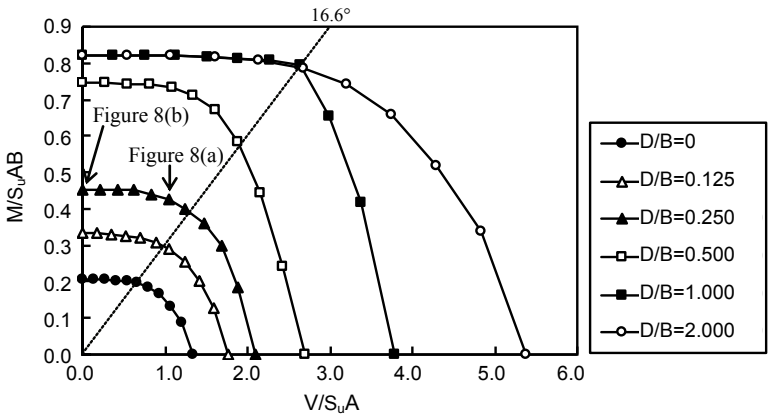

Fig. 7 Failure Envelopes in M-V Space (c_b/c_t=0.25)

Figures 8(a) and 8(b) compare the displacement fields between a combined loading with positive vertical and positive moment (a) and the pure positive moment loading (b). The displacement fields suggest that critical failure mode changes from the wedge mode to the scoop rotational mode. The depth of rotational surface extends to 80% of the footing width.

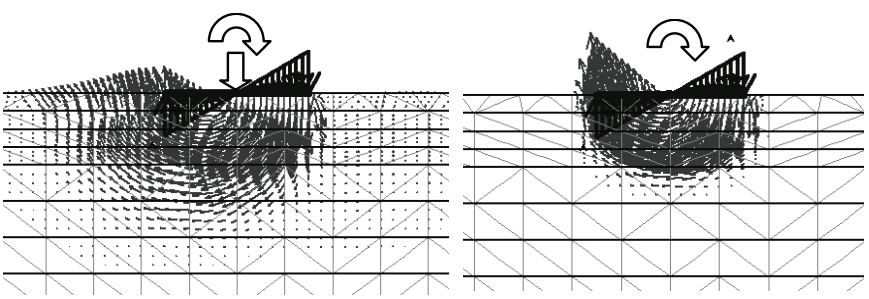

(a) Positive Vertical and Positive Moment Loading (Scale Factor=2)

(b) Pure Positive Moment Loading (Scale Factor=1)

Fig. 8 Failure Mode (D/B=0.25, c_b/c_t=0.25)

The normalized form of V-M failure envelop is presented in Figure 9. All failure envelops for various D/B values can be plotted almost on a single curve except for the case of D/B=1.0, in contrast to V-H plane. Figure 10 plots the value of M/s_uAB against H/s_uA for various values of D/B in the range from 0 to 2.0 for the case of c_b/c_t=0.25. It is noted that moment capacity slightly increases with application of horizontal load for the case of single layer (D/B=2.0 and 0), whereas moment capacity slightly decreases with application of horizontal load for other cases. As will be seen later, however, the decrease in moment capacity with increasing horizontal load is observed only for the cases of c_b/c_t value being small.

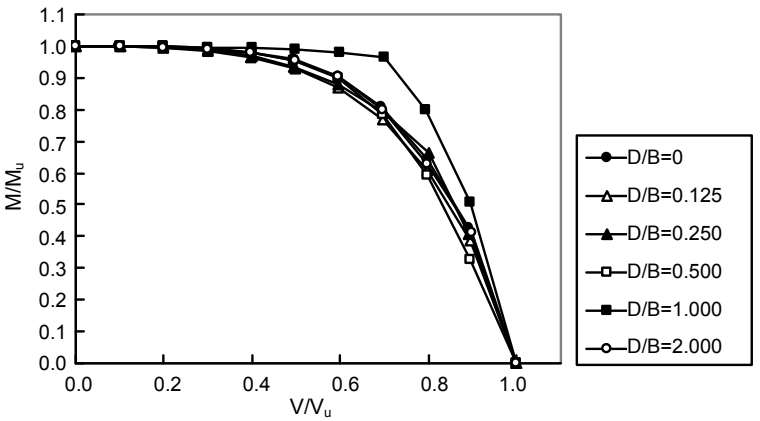

Fig. 9 Normalized Failure Envelopes in M-V Space (c_b/c_t=0.25)

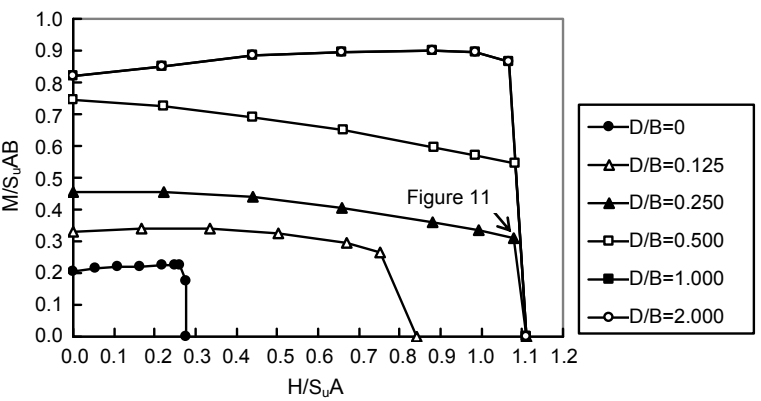

Fig. 10 Failure Envelopes in M-H Space (c_b/c_t=0.25)

Figure 11 shows the displacement field for the case of positive moment and positive horizontal loading. The failure mode seems to belong to the scoop rotational mode. The depth of rotational surface extends to a depth of 100% of the footing width which may be compared with 60% in Figure 8(b).

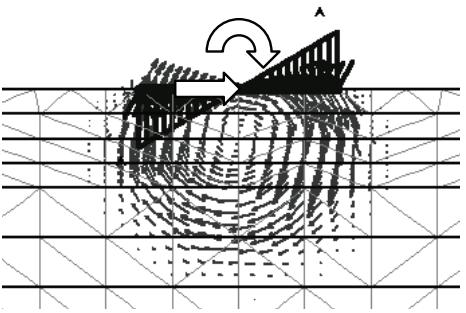

Fig. 11 Failure Mode (D/B=0.25, c_b/c_t=0.25, Scale Factor=0.5)

The normalized form of H-M failure envelop is presented in Figure 12, where all failure envelops are plotted inside that of single layer.

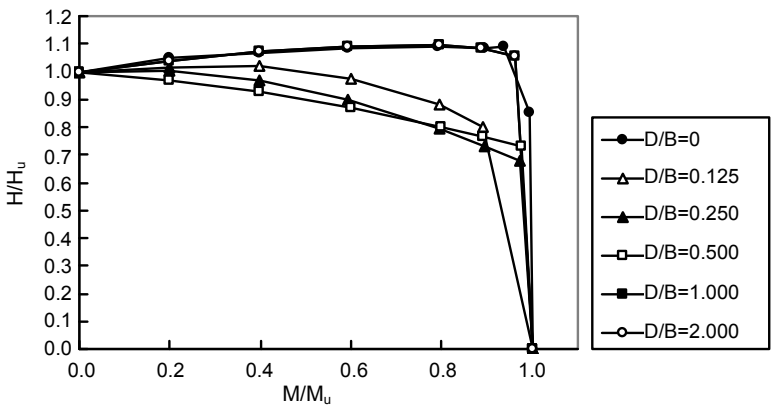

Fig. 12 Normalized Failure Envelopes in M-H Space (c_b/c_t=0.25)

Effect of c_b/c_t Value

In order to examine the effect of c_b/c_t value, Figure 13 shows the cases of c_b/c_t= 0.75. It is apparent by comparing with Figures 4, 7 and 10 that the smaller value of c_b/c_t significantly influences the shape of failure surface than the larger value of c_b/c_t does. The effect of c_b/c_t is more marked in M-H plane. In contrast to Figure 10, Figure 13 (c) shows that moment capacity slightly increases with the application of horizontal load for all the cases of D/B.

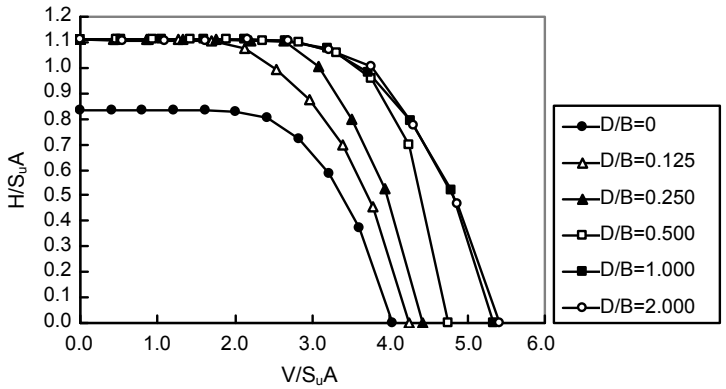

(a) H-V Space

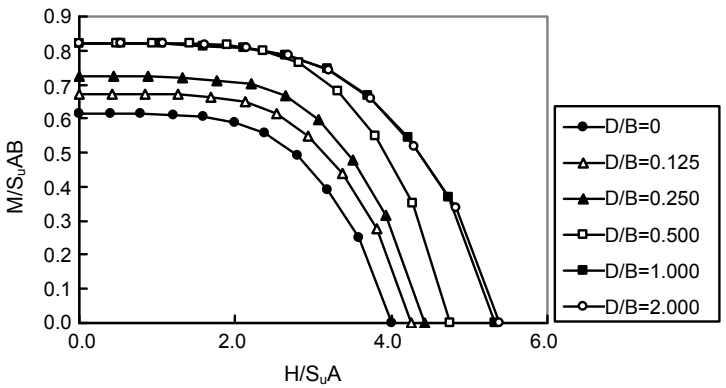

(b) M-V Space

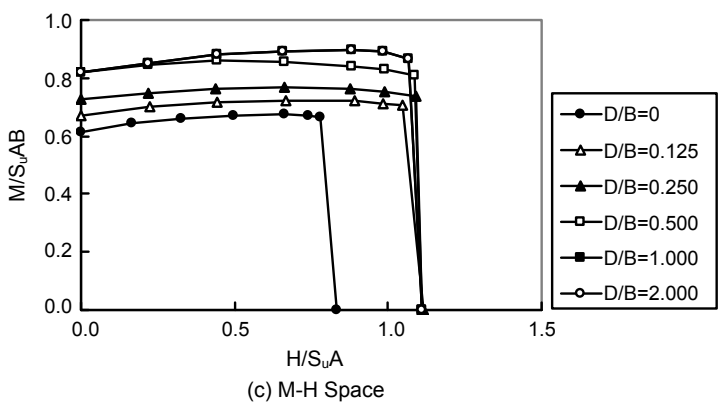

(c) M-H Space

Fig. 13 Failure Envelopes (c_b/c_t= 0.75)

Bearing Capacity of Footing on Soft Clay Overlying Stiff Clay $c_b/c_t>1$

Failure Surface on V-H Plane

Figure 14 plots the value of H/s_uA against V/s_uA for various values of D/B in the range from 0 to 2.0 for the case of $c_b/c_t=2.0$. For the case of D/B=0 (uniform undrained shear strength of c_b), the vertical bearing capacity (V_u) gradually decreases with increasing D/B value. But the horizontal bearing capacity (H_u) suddenly drops to a half when D/B changes even from 0 to 0.125, indicating that the existence of thin soft layer drastically changes the horizontal bearing capacity. If a thin layer of soft clay exists on the top layer, the horizontal resistance (H_u) is governed by the value of c_t, whereas the vertical bearing capacity (V_u) is less sensitive to the existence of thin soft layer. The values for D/B from 0.125 to 2.0 are identical to those of D/B=2.0 until the angle of loading inclination, defined by $\tan^{-1}(H/V)$ becomes around 18.7°. Normalized failure envelops for 0<D/B<2.0 are located within those of the single clay layer, as is seen in Figure 15.

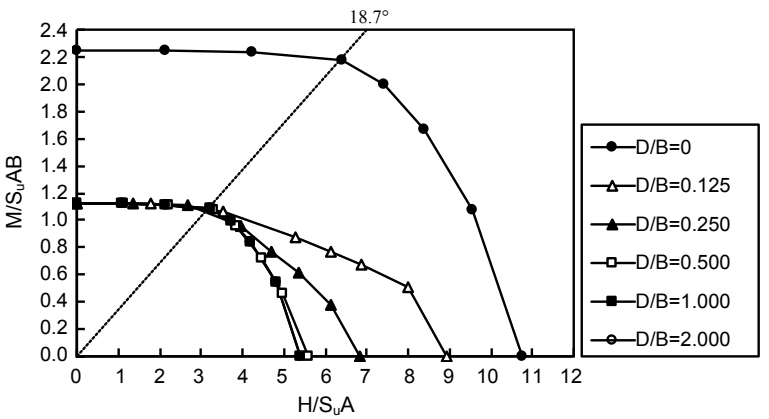

Fig. 14 Failure Envelopes in H-V Space ($c_b/c_t=2.0$)

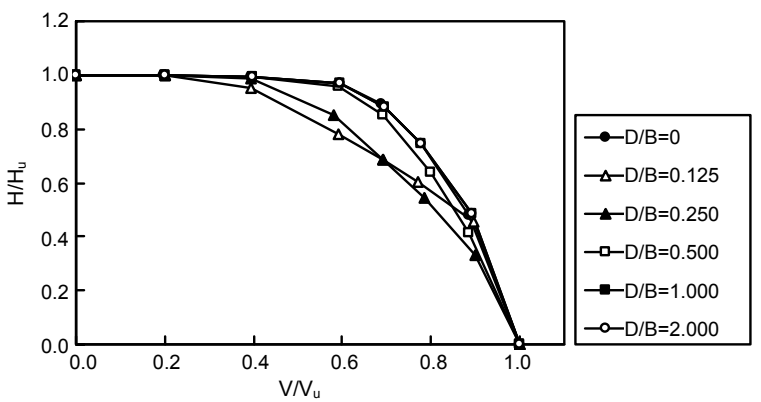

Fig. 15 Normalized Failure Envelopes in M-H Space ($c_b/c_t=2.0$)

Failure Surfaces on V-M Plane and H-M Plane

Figure 16 plots the value of M/s_uAB against V/s_uA for various values of D/B in the range from 0 to 2 for the case of c_b/c_t=2.0. It can be seen that the failure surface gradually becomes smaller as D/B increases. Similar to V-H plane, normalized failure envelops for 0<D/B<2.0 are located within those of the single clay layer, as is seen in Figure 17. It should be noted here that there is a slight difference between the values of D/B=0.0 and 2.0. Figure 18 plots the value of M/s_uAB against H/s_uA for various values of D/B in the range from 0 to 2.0 for the case of c_b/c_t=2.0. In this series of analysis, the combined loading with positive moment and negative horizontal load was also considered. It is noted that the shape of interaction diagram of positive moment and positive horizontal loading significantly differ from that of positive moment and negative moment loading. Application of negative horizontal load results in gradually drops of moment capacity, whereas positive horizontal loads lead to slightly increase in moment capacity. This result is consistent with the results by Bransby and Randolph (1998) and Taiebat and Carter (2000).

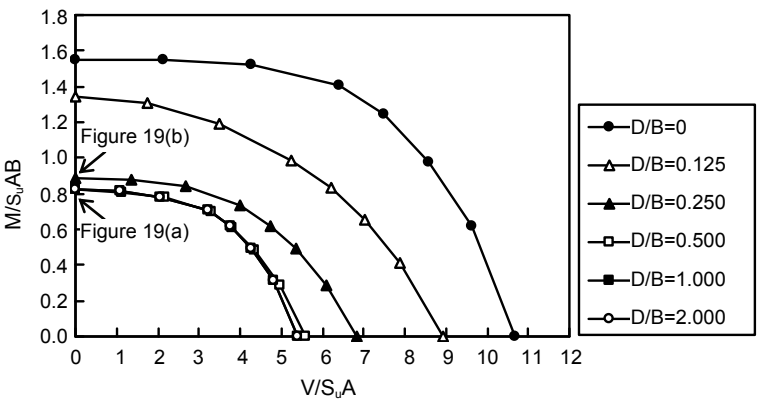

Fig. 16 Failure Envelopes in M-V Space (c_b/c_t=2.0)

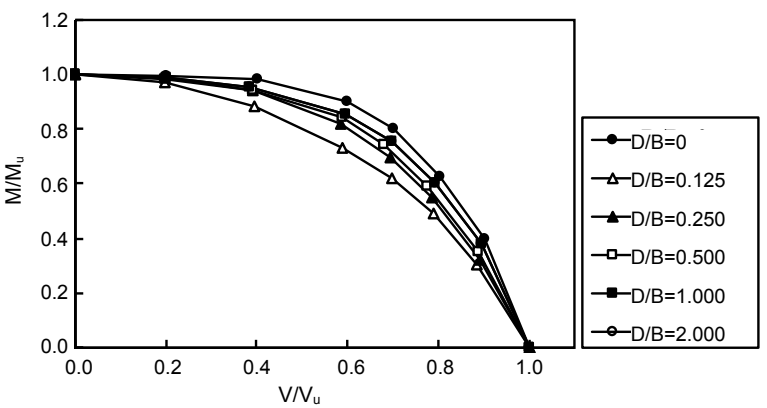

Fig. 17 Normalized Failure Envelopes in M-V Space (c_b/c_t=2.0)

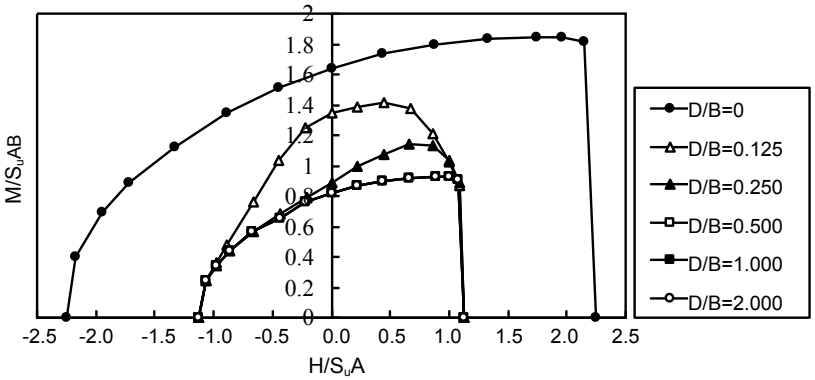

Fig. 18 Failure Envelops in M-H Space (c_b/c_t=2.0)

Figure 19 shows the displacement fields for pure moment loading in the case of D/B=0.25 and 0.5, indicating that the failure mode is localized in the top soft layer. Figure 20 presents the normalized failure envelops.

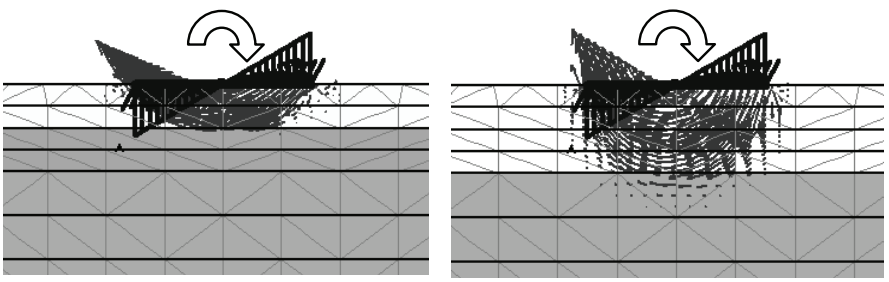

(a) D/B=0.25 (Scale Factor=10) (b) D/B=0.50 (Scale Factor=0.25)

Fig. 19 Failure Mode (c_b/c_t=2.0)

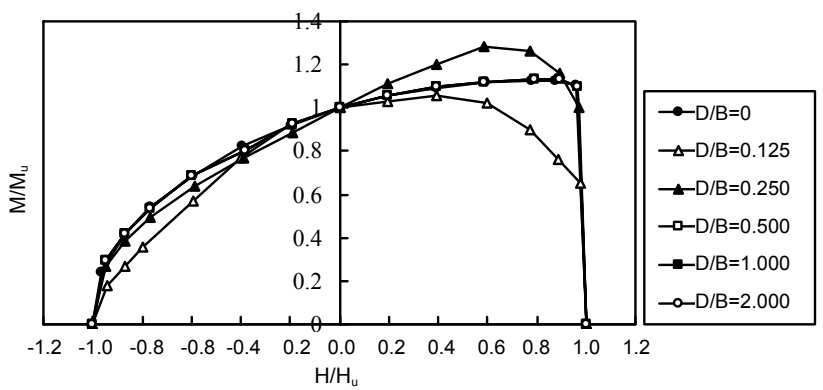

Fig. 20 Normalized Failure Envelopes in M-H Space (c_b/c_t=2.0)

Evaluation of bearing capacity

Failure Surface

As have been discussed, the thin soft clay in the top layer sensitively influences on the shape of failure surface, which poses a difficulty in developing a simple yet practical proposal for an equation describing failure surface. An attempt was made, therefore, to develop equations only for the cases of footing on stiff clay overlying soft clay. Taiebat and Carter (2000) proposed the equation for failure surface of footing under combined loading and suggested to use α=0.3 in Equation (1), which gives a reasonable value for single layer. As have been previously discussed, the modification is required to accommodate the effect of c_b/c_t and D/B on the failure surface in M-H plane as,

For c_b/c_t<1

$$\alpha = 0.25 - 1.45\frac{D}{B}\left(\frac{c_b}{c_t} - 0.84\right) \text{ when D/B<1.0 and } c_b/c_t < 0.84, \text{ MH>0} \quad (2)$$

$$\alpha = 0.25 \text{ when D/B>1.0 or } c_b/c_t > 0.84, \text{ MH<0} \quad (3)$$

Bearing Capacity Charts

Figure 21 presents the chart for vertical bearing capacity factor. As mentioned before, the present study gives about 5% larger values than the plastic solution of (2 + π).

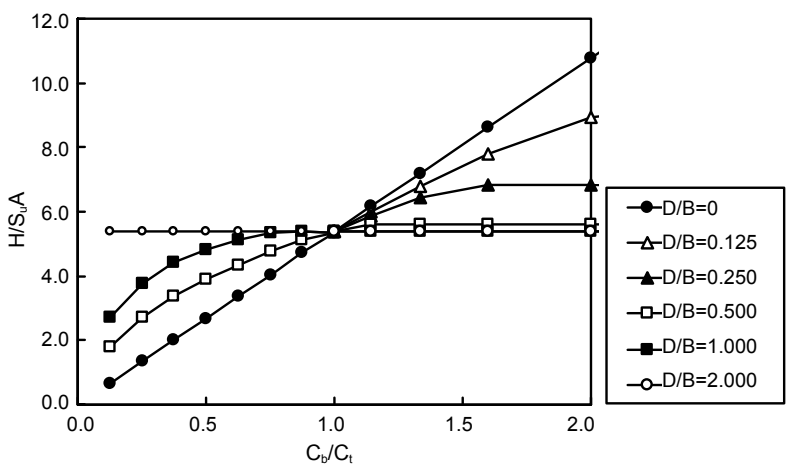

Fig. 21 Chart for Vertical Capacity Factor

For c_b/c_t<1

$$\frac{V_u}{s_u A} = 5.34\left\{1-\left(1-\frac{c_b}{c_t}\right)\left(1-0.5\frac{D}{B}\right)\right\} \le 5.34 \quad (4)$$

For $c_b/c_t>1$

$$\frac{V_u}{s_u A} = 5.34\left\{1+\left(\frac{c_b}{c_t}-1\right)\left(1-2.0\frac{D}{B}\right)\right\} \ge 5.34 \quad (5)$$

As was pointed out, the horizontal bearing capacity was highly sensitive to the strength of top clay layer. As is seen in Figure 22 showing the chart of horizontal capacity, horizontal capacity is proportional to the strength ratio, c_b/c_t for the case of D/B=0.0 and is constant regardless of c_b/c_t for the cases of D/B more than 0.25. Only the situations where c_b/c_t being less than 0.75 and D/B = 0.125, need to consider nonlinearity. The following equations are proposed for practical use.

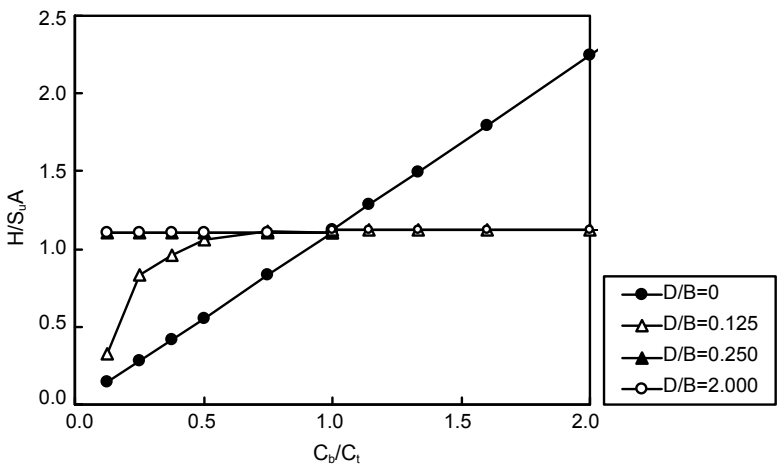

Fig. 22 Chart for Horizontal Capacity Factor

For $c_b/c_t<1$

$$\frac{H_u}{s_u A} = \frac{c}{s_u A} \qquad \begin{cases} c = c_t & D/B > 0.25 \\ c = c_b & D/B < 0.25 \end{cases} \quad (6)$$

For $c_b/c_t>1$

$$\frac{H_u}{s_u A} = \frac{c_t}{s_u A} \quad (7)$$

Figure 23 shows the chart for moment capacity factor. The following equations can fit the analytical results and is proposed to use for practical purposes.

For $c_b/c_t<1$

$$\frac{M_u}{s_u AB} = 0.82\left\{1-\left(1-\frac{c_b}{c_t}\right)\left(1-1.33\frac{D}{B}\right)\right\} \le 0.82 \quad (8)$$

For $c_b/c_t>1$

$$\frac{M_u}{s_u AB} = 0.82\left\{1+\left(\frac{c_b}{c_t}-1\right)\left(1-3.5\frac{D}{B}\right)\right\} \ge 0.82 \quad (9)$$

Care must be exercised in extrapolating the equations beyond the value of c_b/c_t more than 2.0.

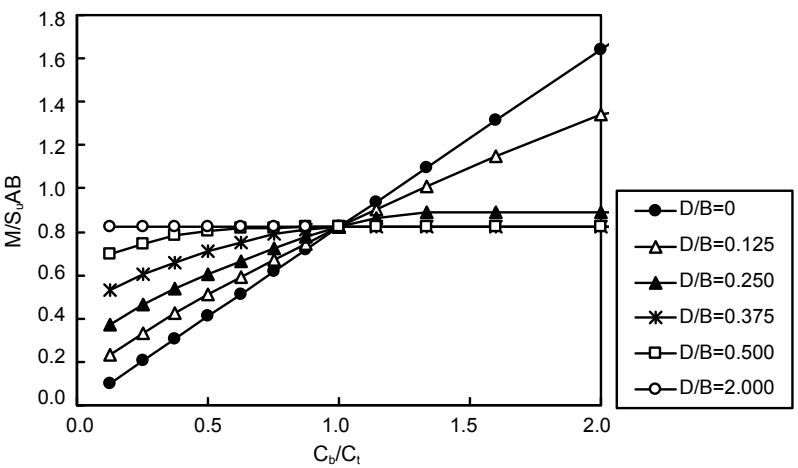

Fig. 23 Chart for Moment Capacity Factor

Conclusions

A series of FEM analyses were conducted to examine the bearing capacity of strip footing on two-layer clay deposits subjected to combined loading. The following conclusions were drawn.

- There exists a critical depth above which the bearing capacity is affected by the bottom layer. When the top layer is as thick as twice the footing width, the existence of bottom layer practically can be ignored.
- The existence of thin soft top layer causes significant influence on the bearing capacity, in particular on horizontal capacity.
- The effect of two-layer clay deposit on bearing capacity is more marked for smaller values of strength ratio, c_b/c_t.
- Non-symmetric failure envelops are obtained in horizontal load and moment plane even for two layered clay deposits, depending upon the sign convention of horizontal load and moment.

- Charts for bearing capacity are presented for various combinations of D/B and c_b/c_t, together with simple yet practical equations for evaluation of bearing capacity.

References

Bolton, M. (1979): *A Guide to Soil Mechanics*, London, MacMillan, pp. 323-324.

Bransby, M. F. and Randolph, M. F. (1998): 'Combined loading of skirted foundation', *Geotechnique*, 48(5), pp. 637-655.

Brinkgreve, R.B.J. (2002): *PLAXIS 2D-version 8*, Delft University of Technology & PLAXIS b.v., The Netherlands.

Brown, J. D. and Meyerhof, G. G. (1969): 'Experimental study of bearing capacity in layered clays', *Proc. of 7th International Conference on Soil Mechanics and Foundation Engineering*, Vol.2, pp. 45-51.

Button, S. J. (1953): 'The bearing capacity of footings on a two-layered cohesive subsoil', *Proc. of 3rd International Conference on Soil Mechanics and Foundation Engineering*, Vol.1, pp. 332-335.

Chen, W. F. (1975): *Limit Analysis and Soil Plasticity*, Elsevier, Amsterdam, The Netherlands.

Florkiewicz, A. (1989): 'Upper bound to bearing capacity of layered soil', *Canadian Geotechnical Journal*, 26(4), pp. 730-736.

Hanna, A. M. (1981): 'Foundations on strong and overlying weak sand', *Journal of Geotechnical Engineering Division.*, *ASCE*, 107(GT7), pp. 916-927.

Kim, J. K., Yang, T. S., Baek, W. J. and Lee, S. (2008): 'Estimating bearing capacity for dredged and reclaimed ground', *Proc. of 6th Asian Young Geotechical Engineers Conference*, pp. 240-250.

Merifield, R. S., Sloan, S. W. and Yu, H. S. (1999): 'Rigorous plasticity solutions for the bearing capacity of two layered clays', *Geotechnique*, 49(4), pp. 471-490.

Meyerhof, G. G. and Hanna, A. M. (1978): 'Ultimate bearing capacity of foundations on layered soils under inclined load', *Canadian Geotechnical Journal*, 15(4), pp. 565-572.

Meyerhof, G. G. (1953): 'The bearing capacity of foundations under eccentric and inclined loads', *Proc. of 3rd International Conference on Soil Mechanics and Foundation Engineering*, Vol. 1, pp. 440-445.

Michalowski, R. L. and Shi, L. (1995); 'Bearing capacity of footings over two-layer foundation soils', *Journal of Geotechnical Engineering Division*, ASCE, 121(5), pp. 421-427.

Michalowski, R. L. (2002): 'Collapse loads over two-layer clay foundation soil', *Soils and Foundations*, 42(1), pp. 1-7.

Nakase, A., Kimura, T., Saitoh, K., Takemura, J. and Hagiwara, T. (1987): 'Behaviour of soft clay with a surface crust', *Proc. of 8th Asian Regional Conference on Soil Mechanics and Foundation Engineering*, Vol. 1, pp. 401-404.

Purshothamaraj, P., Ramiah, B.K. and Rao, K.N.V. (1974): 'Bearing capacity of strip footings in two layered cohesive-frictional soils', *Canadian Geotechnical Journal*, 11(32), pp. 32-45.

Reddy, A.S. and Srinivasan, R.J. (1967): 'Bearing capacity of footings on layered soils', *Soil Mechanics and Foundation Engineering Division*, *ASCE*, 93(SM2), pp. 83-99.

Taiebat H. and Carter J.P. (2000): 'Numerical studies of the bearing capacity of shallow footings on cohesive soil subjected to combined loading', *Geotechnique*, 50 (4), pp. 409-418.

Wang, C. X., and Carter, J. P. (2002): 'Deep penetration of strip and circular footings into layered clays'. *International Journal of Geomechanics*, 2(2), pp. 205-232.

Zhu, M. and Michalowski, R.L.(2005): 'Shape factors for limit loads on square and rectangular footings'. *Journal of Geotechnical and Geoenvironmental Engineering*, ASCE, 131(2), pp. 223-231